RAPID REPORT

Reduced low-voltage activated K^+ conductances and enhanced central excitability in a congenitally deaf (*dn/dn*) mouse

Richardson N. Leao[1], Amy Berntson[1], Ian D. Forsythe[2] and Bruce Walmsley[1]

[1] *Synapse and Hearing Laboratory, The John Curtin School of Medical Research, The Australian National University, Canberra, ACT 0200, Australia*
[2] *Department of Cell Physiology and Pharmacology University of Leicester, PO Box 138, Leicester LE1 9HN, UK*

We have investigated changes in the neuronal excitability of the auditory brainstem in a congenitally deaf mouse (*deafness dn/dn*). Whole cell patch recordings from principal neurones of the medial nucleus of the trapezoid body (MNTB) showed strikingly enhanced excitability in the deaf mice when compared to control CBA mice at 12–14 days postnatal. MNTB neurones in normal CBA mice showed the phenotypic single action potential response on depolarization in current clamp; however, recordings from CBA mice carrying the homozygous *deafness* mutation fired trains of action potentials on depolarization. We show here that these changes are associated with reduced functional expression of dendrotoxin-sensitive Kv1 potassium channels. In contrast, no differences were found in voltage-gated calcium currents between control and deaf mice. These results reveal that loss of hair cell function in the cochlea leads to changes in ion channel expression in the central nervous system and suggests that this deafness model will be an important tool in understanding central changes occurring in human congenital deafness and in exploring activity-dependent regulation of ion channel expression.

(Received 2 May 2004; accepted after revision 28 June 2004; first published online 2 July 2004)
Corresponding author B. Walmsley: Synapse and Hearing Laboratory, Division of Neuroscience, John Curtin School of Medical Research, Australian National University, PO Box 334, Canberra, ACT 0200, Australia. Email: bruce.walmsley@anu.edu.au

Many forms of congenital deafness result from cochlea dysfunction (Steel, 1995), without obvious primary defects in central auditory pathways. However, aberrant auditory activity during development is likely to have many secondary consequences for central connectivity (Friauf & Lohmann, 1999; Rubel & Fritzsch, 2002). Activity-dependent mechanisms are important in regulating both synaptic strength and the intrinsic membrane properties of postsynaptic neurones (Desai *et al.* 1999; Davis & Bezprozvanny, 2001; Cohen-Cory, 2002). Cochlear ablation (mechanically or chemically induced) changes the morphological and functional properties of brainstem auditory neurones (Friauf & Lohmann, 1999; Francis & Manis, 2000; Rubel & Fritzsch, 2002; Vale & Sanes, 2002; Vale *et al.* 2003), but very few studies have examined the effects on the intrinsic membrane properties of these neurones (Francis & Manis, 2000). Surprisingly, there is virtually no information on the detailed synaptic and neuronal membrane properties in central auditory pathways of naturally occurring models of congenital deafness during development.

In the present study, we have investigated a congenitally deaf mutant mouse (*dn/dn*), caused by dysfunctional hair cells, rather than a nervous system defect (Bock *et al.* 1982; Keats & Berlin, 1999). The *dn/dn* mouse is a naturally occurring strain with a recessive mutation of *Tmc1* (transmembrane cochlear-expressed gene 1; Kurima *et al.* 2002). *Tmc1* mRNA is confined to the cochlea, and is not detectable above background levels in the brain. The *Tmc1* mutation results in an absence of auditory nerve activity from the earliest stages of postnatal development, before ear canal opening in the mouse (A. Paolini, M. Youssoufian, A. Berntson & B. Walmsley, unpublished observation). Previous studies show enhanced excitatory synaptic current amplitude in the ventral cochlear nucleus (Oleskevich & Walmsley, 2002) and altered inhibitory transmission in the medial nucleus of the trapezoid body (MNTB) (Leao *et al.* 2004). In this study, we have examined the effects of congenital deafness on post-synaptic membrane properties in principal neurones of the MNTB. MNTB neurones receive a single large calyceal excitatory synapse (the calyx of Held) from globular bushy

 DOI: 10.1113/jphysiol.2004.067421

cells in the anteroventral cochlear nucleus, which in turn receive their input directly from the auditory nerve (Friauf & Lohmann, 1999). The calyx of Held has been extensively investigated over recent years as a model central excitatory synapse (Schneggenburger *et al.* 2002). Its giant excitatory postsynaptic current (EPSC) coupled with distinctive postsynaptic cell membrane properties and other adaptations act to preserve the timing and pattern of auditory signalling across the auditory brainstem, required for accurate sound localization (Wu & Kelly, 1993). MNTB neurones express a suite of voltage-gated potassium conductances which regulate their excitability, including high-threshold Kv3.1 channels that are important in minimizing action potential duration and ensuring phase locking (Wang *et al.* 1998). Another crucial intrinsic current determining MNTB neuronal firing properties is the low-threshold voltage-gated potassium current (I_{LT}), which activates close to resting membrane potentials (Coetzee *et al.* 1999) and is mediated by Kv1 channels containing dendrotoxin (DTX)-sensitive subunits, namely Kv1.1, Kv1.2 or Kv1.6 (Brew & Forsythe, 1995; Dodson *et al.* 2002). These I_{LT} currents serve to increase the membrane conductance, raise threshold for action potential generation and minimize multiple firing. The response of MNTB neurones to a sustained depolarizing current step is the firing of a single, or sometimes two to three, action potentials (Brew & Forsythe, 1995; Dodson *et al.* 2002). We have examined the membrane properties of MNTB neurones in congenitally deaf and normal mice. Our results from deaf mice show striking differences in the membrane properties of MNTB neurones at voltages close to firing threshold, suggesting that these neurones respond to altered presynaptic activity by selectively regulating the postsynaptic expression of specific voltage-gated channels to significantly increase neuronal excitability.

Methods

MNTB slice electrophysiology

Normal (CBA, 12–14 days postnatal) and congenitally deaf (*dn/dn* with CBA background, 12–14 days postnatal) mice were decapitated according to the Australian National University Animal Ethics Committee protocol. The forebrain and cerebellum were removed and placed in ice-cold low-calcium artificial cerebrospinal fluid (ACSF; mM: 130 NaCl, 3.0 KCl, 5.0 $MgCl_2$, 1.0 $CaCl_2$, 1.25 NaH_2PO_4, 26.2 $NaHCO_3$, 10 glucose, equilibrated with 95% O_2, 5% CO_2). Transverse slices (150 μm) were made of the medial nucleus of the trapezoid body (MNTB) using an Electron Microscopy Sciences (EMS) (Fort Washington, PA, USA) oscillating tissue slicer. Slices were incubated for 1 h in normal ACSF (mM: 130 NaCl, 3.0 KCl, 1.3 Mg_2SO_4, 2.0 $CaCl_2$, 1.25 NaH_2PO_4, 26.2 $NaHCO_3$, 10 glucose, equilibrated with 95% O_2, 5% CO_2) at 35°C and subsequently held at room temperature (22–25°C) for electrophysiological recording.

Whole-cell current-clamp and voltage-clamp recordings from visualized MNTB neurones were made using Axopatch 1D or Multiclamp 700A amplifiers (Axon Instruments, Union City, CA, USA). Current-clamp recordings were performed with an Axopatch 1D. Distortion of action potential waveforms would have been the same for MNTB cells in normal and deaf mice, and minimal due to the (similar) low cell resistance (150–200 MΩ), high cell capacitance (approximately 30 pF) and simple single compartment electrotonic cell morphology. Electrode resistance was typically 4 MΩ and series resistance (< 10 MΩ) was routinely compensated by > 80%. Data analysis was performed using Axograph (Axon Instruments) and MATLAB R13 (The Mathworks, Inc., Natick, MA, USA) software.

Potassium current measurements and analysis

Patch electrodes for current-clamp and voltage-clamp recordings contained (mM): 122.5 potassium gluconate, 17.5 KCl, 9 NaCl, 1 $MgCl_2$, 10 Hepes, 3 Mg-ATP, 0.3 GTP-tris and 0.2 EGTA. The pH was adjusted to 7.2 using KOH, and the osmolarity, when necessary, adjusted to 290–300 mosmol l^{-1} with sorbitol. Electrode resistance averaged 4.5 MΩ and series resistance < 10 MΩ. For experiments examining DTX-sensitive currents, the following drugs were added to the perfusate: (1 μM TTX, 10 μM ZD7288 (Tocris Cookson Ltd, Bristol, UK) to block I_h, 50 μM $CdCl_2$, with and without 100 nM α-DTX). The protocol for applying voltage steps was as follows. The cell was held at a resting potential of −60 mV, which was stepped to a holding pre-potential of −80 mV for 750 ms before the test voltage step to remove potential activation of low threshold currents at −60 mV. Test steps were then made to potentials of −100 mV to +40 mV (in increments of 10 mV) and the current responses measured. Current–voltage relationships were plotted with and without DTX. TTX and α-DTX were obtained from Alomone Laboratories (Israel). Drugs were applied for 15 min before measurements were used in the analysis.

Calcium and barium current measurements

MNTB cells were voltage-clamped at a holding potential of −60 mV. Calcium and barium currents were activated by 200 ms voltage steps from the holding potential to a series of voltages ranging from −100 mV to +40 mV. Patch clamp electrodes were filled with a solution having the following composition (mM): 120 CsCl, 10 NaCl, 40 Hepes, 10 TEA-Cl, 2 Mg_2-ATP, 0.3 Na_3-GTP, 1 EGTA, 2 QX314, pH 7.35. The ACSF was similar to that used in other experiments, but contained 95 mM NaCl

and 30 mM TEA-Cl to block potassium currents. For the pharmacology experiments, barium currents were recorded by replacing 2 mM $CaCl_2$ with 5 mM $BaCl_2$. The following calcium channel blockers were obtained from Sigma (St Louis, MO, USA), and were bath applied: 10 mM nifedipine, 2 μM ω-conotoxin GVIA, 20 nM ω-agatoxin IVA. Nifedipine was continually applied until steady state was reached. Subsequent drugs were added sequentially in combination with nifedipine. All measurements were performed after a steady state had been reached (~3–4 min after drug application). A calcium-free ACSF containing 2 mM $CoCl_2$ was added at the end of the experiment to determine the magnitude of unblocked current.

Student's t test was used to test significant differences between two population means, with $P \leq 0.05$ as a level of significance.

Results

Cell excitability is increased in deaf mice

The firing characteristics of MNTB neurones in deaf and normal mice were investigated by injecting long duration current pulses under current-clamp whole-cell recording of membrane potential. Figure 1 shows typical changes in membrane potential of MNTB neurones when a series of depolarizing current steps was injected (800 ms duration). In MNTB neurones from normal mice (Fig. 1*A*), positive current steps smaller than 150 pA generally caused a small depolarization that decayed quickly to a steady state for the remainder of the current step. Current steps above current threshold (> 150 pA, 800 ms) caused the firing of a single short latency action potential (AP), but injection of much larger currents (> 250 pA) could cause two to five (mean = 1.7) short latency APs in some mouse MNTB neurones during the first 10 ms of the step (with no further APs for the remainder of the pulse (see also Brew *et al.* 2003). The responses of MNTB neurones from deaf mice were strikingly different and more variable than those found in normal mice. The majority of MNTB neurones from deaf mice had lower current thresholds (at least one AP) and fired multiple APs (15–25) during the first half of the current step. For normal mice, 60% of the cells fired at least one AP with 100 pA and 85% with 150 pA, whereas for deaf mice, 53% of the cells fired with 50 pA, 84% with 100 pA and 100% with 150 pA current steps. A typical pattern for MNTB neurones in deaf mice is illustrated in Fig. 1*A* (lower panel). Within this group, some cells ($n = 8$) displayed a decrease in the number of APs (mean = 17.5 ± 0.5 for 150 pA) when the current reached large values (mean = 11.8 ± 0.6 for 250 pA). Other cells ($n = 7$) responded with multiple continuous firing (10–50 APs) to current steps larger than +50 pA, increasing AP frequency with larger current steps, and a small group of cells ($n = 3$) responded to current injection similarly to that from normal mice. MNTB neurones in deaf and normal mice showed no significant difference in input resistance (normal, 185.1 ± 6 MΩ, $n = 25$ cells; deaf, 178.4 ± 9 MΩ, $n = 25$ cells; $P > 0.05$), cell membrane capacitance (normal, 26.0 ± 0.8 pF, $n = 25$ cells; deaf, 27.0 ± 0.6 pF; $P > 0.05$) or resting membrane potential (normal, −63.7 ± 0.4 mV, $n = 30$ cells; deaf, −65.3 ± 0.5 mV, $n = 30$ cells; $P > 0.05$). There was no significant difference in the first AP peak amplitudes (normal, 76.7 ± 1.7 mV, $n = 25$ cells; deaf, 75.3 ± 1.1 mV, $n = 25$ cells) or half-widths (normal, 0.97 ± 0.02 ms, $n = 25$ cells; deaf, 1.02 ± 0.03 ms, $n = 25$ cells) generated in response to a depolarizing current pulse (Fig. 1*B* and *C*). Both normal and deaf mice showed a similar reduction in amplitude and an increase in half-width for the second action potential (Fig. 1*B* and *C*). For MNTB neurones in deaf mice, which usually generated three or more action potentials in response to a current pulse, there was a further reduction in amplitude and increase in half-width of the last action potential (Fig. 1*B* and *C*). Previous studies have clearly linked high voltage-activated currents, such as Kv3 channels, with rapid AP repolarization (Rudy & McBain, 2001; Wang *et al.* 1998) and AP threshold changes with expression of Kv1 channels (Brew & Forsythe, 1995; Dodson *et al.* 2002). The above data suggest that the difference in firing properties between the normal and deaf mice could be caused by changes in low-voltage-activated currents.

Multiple AP firing in deaf mice is due to a reduced low-voltage-activated potassium current

To test this hypothesis α-dendrotoxin (α-DTX) was used to block I_{LT} (Owen *et al.* 1997). Application of α-DTX (100 nM) increased the number of APs in response to depolarizing current pulses in both normal and deaf mice (Fig. 2*A*). The effect of α-DTX on the mean firing rate for different levels of depolarizing current in MNTB neurones is summarized in Fig. 2*B*. Each graph shows the mean number of APs (measured during the whole 800 ms current step) and it is clear that α-DTX (100 nM) had a much greater effect on firing rate in normal mice, increasing APs by more than 10-fold while the deaf mice showed a smaller twofold increase. The firing rates in the presence of α-DTX for a 200 pA current step in normal and deaf mice were not significantly different (83 Hz and 73 Hz for normal and deaf mice, respectively).

In order to further investigate differences in I_{LT} currents between the two groups, whole-cell voltage clamp recordings were obtained in the presence of TTX, $CdCl_2$ (50 μM) and ZD7288 (10 μM) to block sodium, calcium and I_h currents, respectively. The cell membrane potential was held at −60 mV and a pre-pulse to −80 mV (duration 750 ms) was followed by voltage steps (500 ms) to a

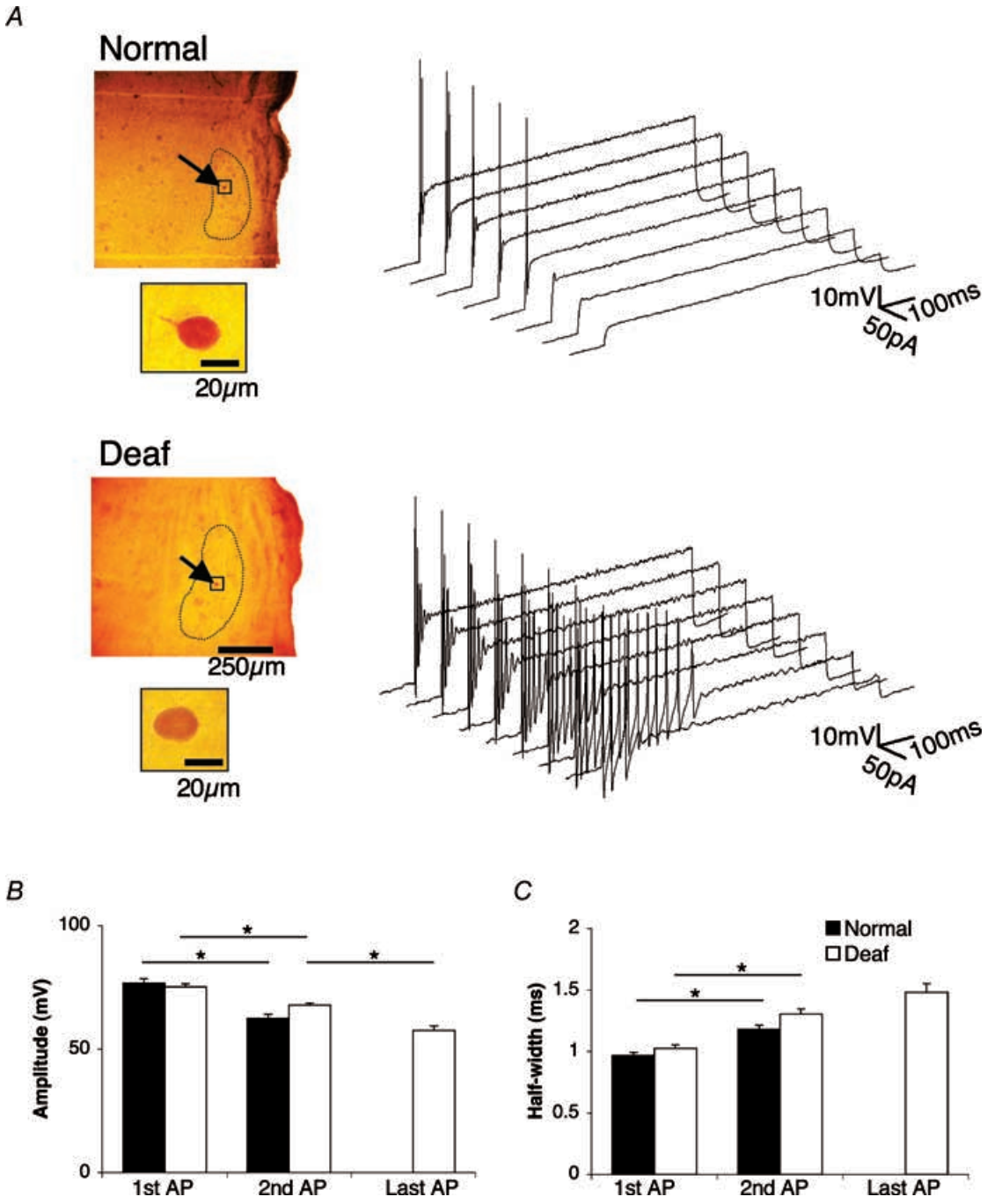

Figure 1. MNTB neurone firing properties differ in deaf mice
A, current clamp recordings from MNTB neurones in CBA mice show the phenotypic single action potential response on depolarization (top) while responses from a deaf mouse are shown below. Depolarizing current pulses, 800 ms duration, were applied in increments of 50 pA, up to 400 pA. MNTB neurones in normal mouse display 1 or 2 spikes on application of suprathreshold currents (> 100 pA). MNTB neurone from a deaf mouse exhibits a lower threshold and fires multiple action potentials to current injection > 50 pA. Left panels illustrate the location of identified MNTB principal cells (arrows), which were recorded and labelled with neurobiotin (insets show the cells at higher magnification). *B*, action potential amplitude shows a similar progressive decline in both normal and deaf mice. Action potential amplitude was measured from a threshold slope (0.25 mV ms^{-1}) to the peak. *C*, the half-width of the action potential in both normal and deaf mice were also similar.

potential that ranged from −100 to + 40 mV. Figure 3*A* illustrates currents recorded in response to voltage steps (from −100 mV to –30 mV) in MNTB neurones from normal and deaf mice, under control conditions (upper traces) and following α-DTX (lower traces). The residual currents following α-DTX are greater in the control records for these examples, reflecting the variability in the residual current between cells (mean relationships are plotted in Fig. 3*C*). Figure 3*Ba* shows currents recorded in response to the full range of voltage steps in MNTB neurones from normal (upper traces) and deaf mice (lower traces). Figure 3*Bb* illustrates an expanded view of current traces (arrows in *Ba*) at a pulse potential of −50 mV for normal and deaf mice. Current–voltage relationships were constructed for each cell (measured 10 ms after the start of the voltage pulse) in the presence and absence of α-DTX (Fig. 3*C*). Figure 3*D* shows the low-threshold α-DTX-sensitive current is much greater for MNTB cells in normal mice compared with deaf mice.

In order to obtain the kinetics of the α-DTX-sensitive current, voltage steps from −100 to +42.5 mV (7.5 mV steps) were applied in MNTB neurones from five normal and five deaf mice (recordings were only accepted if the series resistance before and after α-DTX application did not change by more than 0.5 MΩ). The α-DTX-sensitive current was obtained by subtracting current traces before and after the addition of 100 nM α-DTX. A Boltzmann curve of the form:

$$I/I_{\max} = 1/\left(1 + e^{(V - V_{1/2})/k}\right)$$

was fitted to the α-DTX-sensitive peak currents ($I/I_{\max}$ is the normalized current; V is the voltage; $V_{1/2}$ is the voltage for half-activation and k is the slope). The voltage threshold (at 5% of the current obtained by the Boltzmann fit) for the α-DTX-sensitive current was 55 ± 0.7 mV for normal mice and 42 ± 0.3 mV for deaf mice ($P = 0.04$, $n = 5$). $V_{1/2}$ was 24.7 ± 0.6 mV for normal mice and 16.5 ± 0.8 mV for deaf mice ($P = 0.05$, $n = 5$). Slopes (k) did not differ significantly between normal and

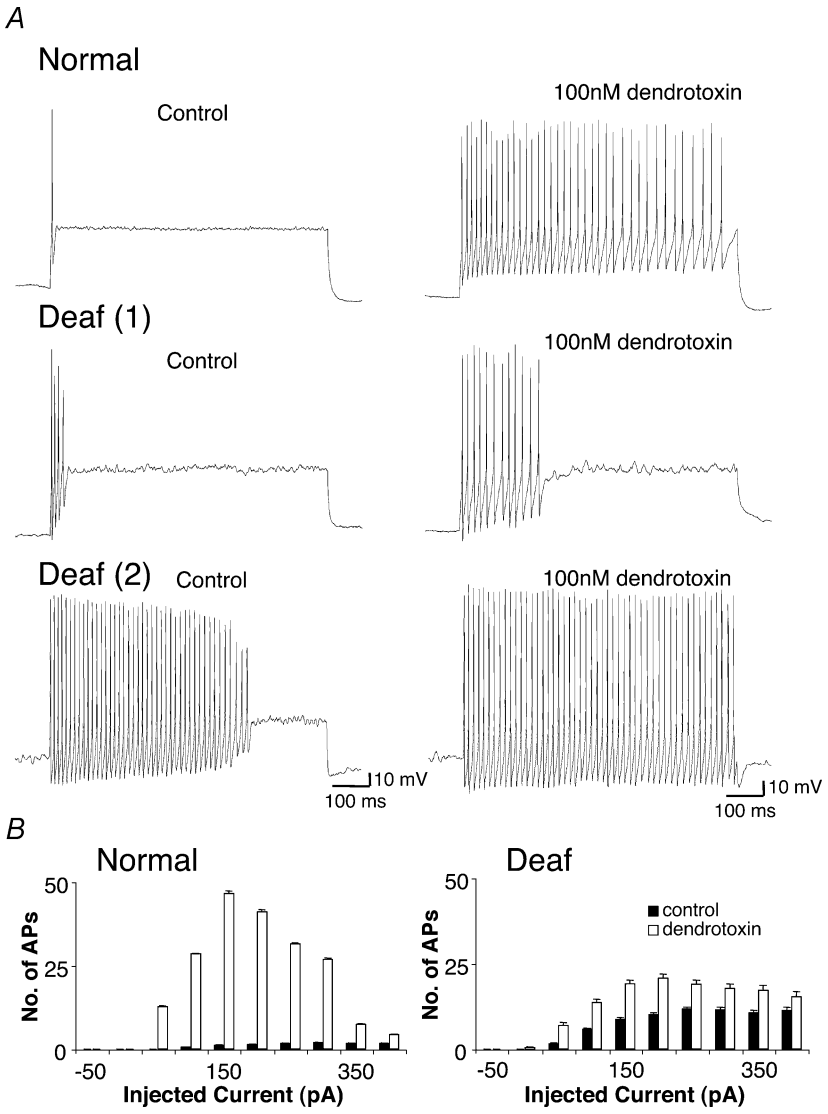

Figure 2. α-Dendrotoxin-sensitive currents contribute to suppression of action potential firing in deaf mice
A, top traces show the response of a MNTB cell from normal mouse before (left) and after (right) the application of α-DTX (current pulse, 150 pA, 800 ms). Lower traces show the responses to the same current injection for two different MNTB cells in deaf mice. *B*, plots of the average action potential number over a range of current steps (duration 800 ms) under control conditions (black bars) and after addition of 100 nM α-DTX (open bars) in normal (left panel) and deaf mice (right panel).

deaf mice (11.6 ± 0.2 mV and 12.1 ± 0.7, respectively). α-DTX-sensitive current activation time constants for normal and deaf mice did not differ significantly at -20 mV (1.7 ± 0.3 ms and 1.9 ± 0.4 ms, respectively; $P > 0.05$, $n = 5$).

Aberrant firing in MNTB neurones from deaf mice in response to synaptic input

In order to investigate the physiological consequences of the different membrane properties of MNTB neurones in deaf mice, the response of MNTB

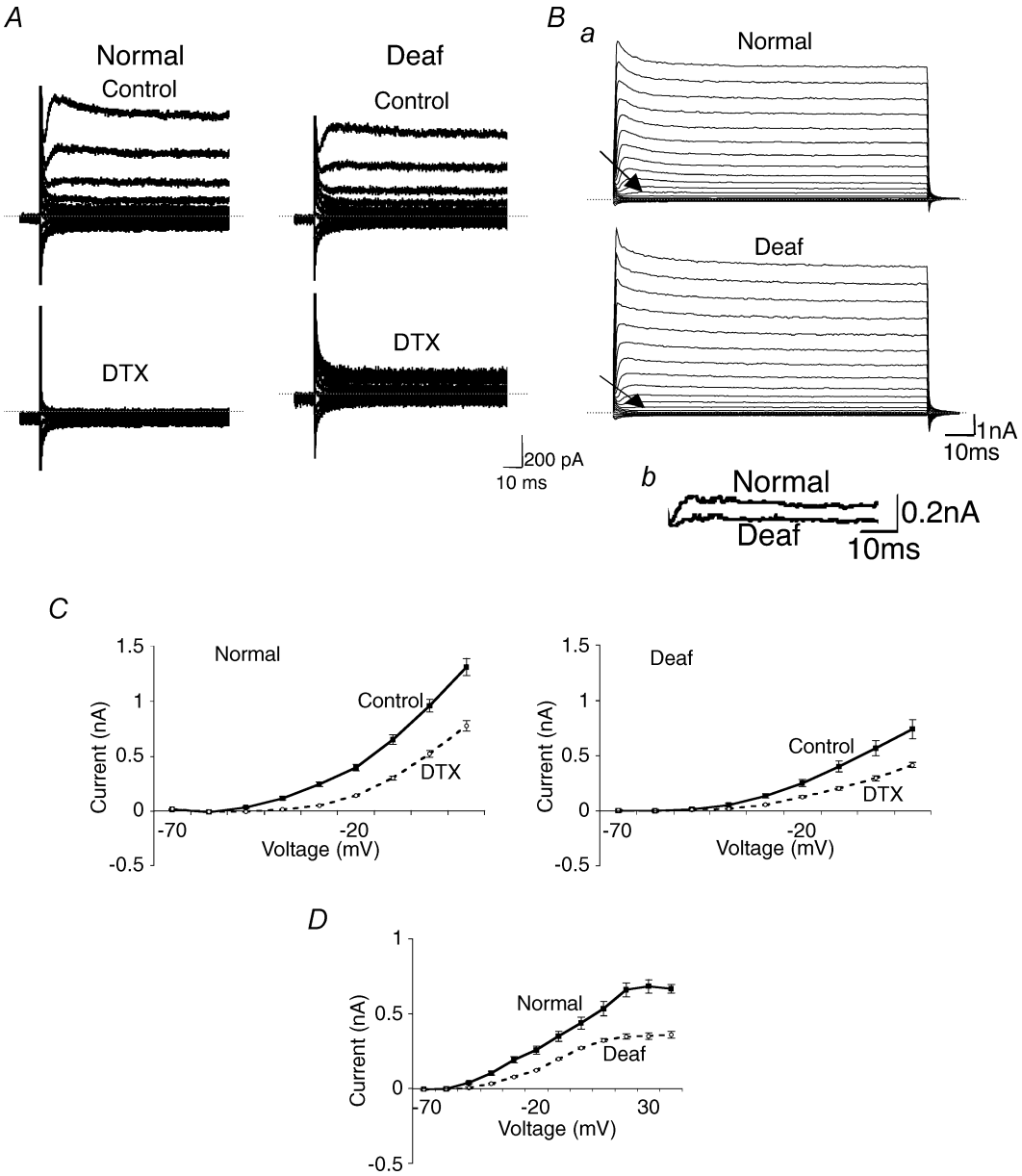

Figure 3. Voltage-clamp recordings of potassium currents in MNTB neurones
A, currents recorded in response to voltage steps (from -100 mV to -30 mV, in increments of 10 mV; prepulse potential -80 mV) in MNTB neurones from normal and deaf mice, under control conditions (upper traces) and following α-DTX (lower traces). *Ba*, currents recorded in response to a larger range of voltage steps (from -100 mV to $+40$ mV, in increments of 10 mV; prepulse potential -80 mV) in MNTB neurones from normal (upper traces) and deaf mice (lower traces). *Bb*, expanded view of current traces (arrows in *Ba*) at a pulse potential of -50 mV for normal and deaf mice. Currents in *A* and *B* not leak-subtracted; dotted line indicates zero current level. *C*, current–voltage relationships for MNTB neurones in normal mice ($n = 9$ cells) and deaf mice ($n = 9$ cells) without DTX (continuous lines) and with α-DTX (100 nM, dashed lines). *D*, α-DTX-sensitive currents (summary; from relationships shown in *B*).

neurones to excitatory synaptic input from the calyx of Held was examined. As shown in Fig. 4*A*, electrical stimulation of afferent fibres produced the characteristic large, fast calyceal synaptic current in MNTB cells from both normal and deaf mice. The voltage response of MNTB neurones to this synaptic current was examined for both single stimuli (left panels) and trains of stimuli (right panels). As illustrated in the current-clamp recordings shown in Fig. 4*A*, single EPSCs produced multiple firing of MNTB neurones in deaf mice, and aberrant (non-synchronized) firing during trains of stimuli. Five out of six cells examined from deaf mice exhibited multiple firing to synaptic input, in marked contrast to the single APs and synchronized firing in MNTB neurones from normal mice (6 out of 6 cells).

Voltage-gated calcium currents are the same in deaf and normal mice

We next recorded calcium currents to investigate if there are differences in another type of voltage-gated current between MNTB neurones from normal and deaf mice. Whole-cell voltage clamp recordings demonstrate that the activation range, and peak amplitude of the calcium currents were the same for normal and deaf mice (normal, -263 ± 59 pA, $n = 9$; deaf, -333 ± 70 pA, $n = 7$, $P > 0.05$). No differences were evident in activation voltage (approx. -40 mV) and voltage of peak inward current (0 mV) between normal and deaf mice (Fig. 4*B*). Peak currents were also the same for normal and deaf mice with barium instead of calcium as the charge carrier (normal, -602 ± 82 pA, $n = 9$; deaf, -586 ± 128 pA, $n = 7$, $P > 0.05$, data not shown). The contribution of each calcium channel type to the whole-cell calcium current was determined by measuring the proportion of the whole-cell current blocked by specific calcium channel blockers. Bath application of the specific calcium channel blockers nifedipine (10 μM), ω-conotoxin GVIA (2 μM) and ω-agatoxin IVA (20 nM) (Fig. 4*C*) demonstrated that there were no significant differences in the proportion of calcium channel subtypes contributing the currents through voltage-gated calcium channels between normal and deaf mice (L-type normal, $14 \pm 5\%$, $n = 4$; deaf, $21 \pm 4\%$, $n = 5$: N-type normal, $30 \pm 4\%$, $n = 7$; deaf $34 \pm 9\%$, $n = 5$: P-type normal, $32 \pm 4\%$, $n = 3$: deaf, $25 \pm 8\%$, $n = 3$: Q/R-type normal $28 \pm 9\%$, $n = 3$: deaf $28 \pm 5\%$, $n = 3$). This is in contrast to a similar study in rat MNTB principal cells where somatic L-type calcium currents were not detected (Barnes-Davies *et al.* 2001). This suggests that, in contrast to voltage-gated potassium currents, voltage-gated calcium currents in MNTB neurones are resistant to modification in congenitally deaf *dn/dn* mice.

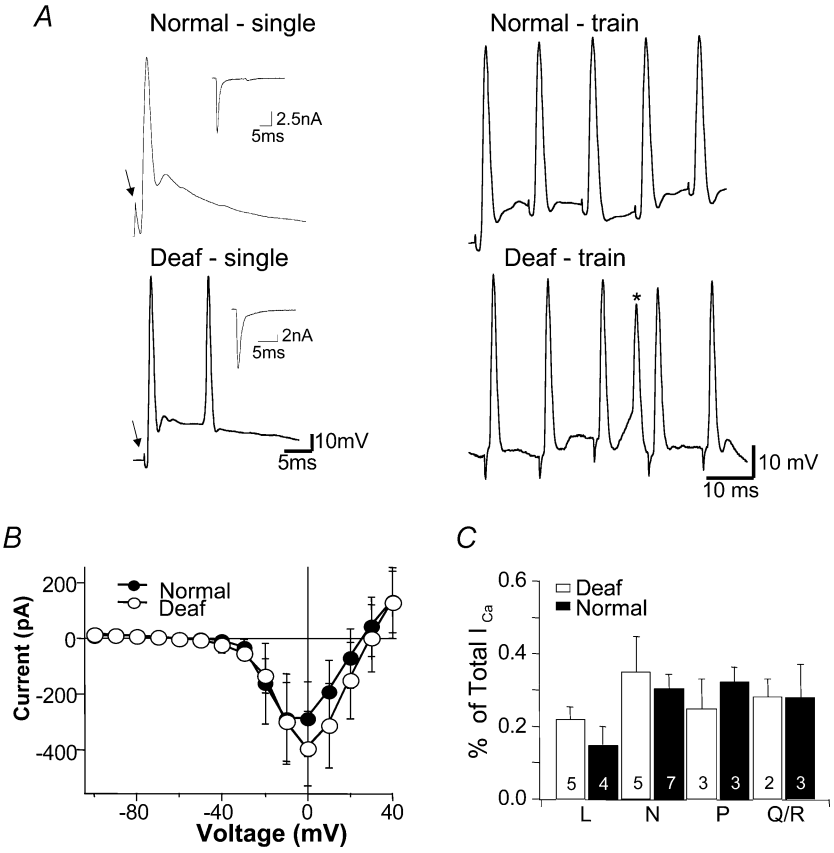

Figure 4. Synaptically evoked firing and calcium currents of MNTB neurones in normal and deaf mice
A, whole-cell voltage clamp recordings of synaptic currents evoked by stimulation of calyceal inputs. Left panels show current clamp recordings of MNTB neurones in response to single stimuli. Right panels show the response of MNTB neurones to trains of stimuli (100 Hz). Note the multiple spikes and aberrant firing of MNTB neurones in deaf mice. *B*, the amplitude, activation range, and peak voltage of activation of the calcium currents of normal mice (open circles) and deaf mice (filled circles) are the same. *C*, pharmacological block of the barium currents of deaf (filled bars) and normal (open bars) mice revealed that they were mediated by the same proportion of calcium channel types. Error bars represent standard deviation.

Discussion

Our results show that loss of auditory input through congenital deafness in the *dn/dn* mouse is associated with specific differences in the intrinsic conductances of central auditory neurones. There is a radical difference in the firing properties of MNTB neurones in deaf mice, with these cells firing multiple or continuous action potential trains on depolarizing current injection, which would clearly disrupt the precision and high frequency following of these cells to presynaptic input. MNTB cells from deaf mice exhibited substantially smaller low-threshold potassium currents near resting potential than in normal mice, due in part to a decreased DTX-sensitive current.

The results of this study provide the first insight into changes of intrinsic conductances and neuronal properties of central pathways in a model of naturally occurring neonatal congenital deafness in which auditory nerve activity is disrupted before the onset of hearing (see von Hehn *et al.* (2004) for a study on a progressive hearing loss mouse model). Interestingly, the amplitude and kinetic properties of voltage-gated calcium currents were similar for MNTB neurones in normal and deaf mice, even at the level of calcium channel subtypes. This demonstrates that there is not a universal change in all voltage-activated channels in deaf mice, and suggests that calcium channel expression in MNTB neurones may be less sensitive than expression of potassium channels to neural activity during development. It is possible, however, that the expression of a variety of other channels is different in the deaf mice, and we are currently exploring this issue. Our results also have implications for more general questions concerning the role of activity during development and in the regulation of synaptic transmission and neuronal membrane properties, suggesting that activity-dependent regulation of intrinsic potassium conductances is an important part of functional development. In this regard, our results fit remarkably well with observations made on tissue-cultured cortical neurones (Desai *et al.* 1999) where exposure of the cultures to TTX (to block activity) resulted in a down-regulation in potassium currents and no change in voltage-gated calcium currents, as observed in our *in vivo* model of a lack of auditory activity. Furthermore, a role for depolarization in regulating potassium channel expression has been directly demonstrated in auditory brainstem neurones (Liu & Kaczmarek, 1998). Previous data from the AVCN endbulb (Oleskevich & Walmsley, 2002) in combination with the present results suggest that both synaptic and intrinsic conductances are under activity-dependent control. Of particular interest is the role of spontaneous activity in the auditory pathway development before hearing onset (Rubel & Fritzsch, 2002) (thought to be one mechanism of regulating synaptic connections) and the recent evidence for regulated expression of Kv1 and Kv3 channels by neurotrophic factors in the spiral ganglion (Mo *et al.* 2002).

Finally, our results may have important implications for cochlear implants, in which it cannot be assumed that the properties of central pathways are normal (Shepherd & Hardie, 2001; Van Hoesel & Tyler, 2003).

References

Barnes-Davies M, Owens S & Forsythe ID (2001). Calcium channels triggering transmitter release in the rat medial superior olive. *Hear Res* **162**, 134–145.

Bock GR, Frank MP & Steel KP (1982). Preservation of central auditory function in the deafness mouse. *Brain Res* **239**, 608–612.

Brew HM & Forsythe ID (1995). Two voltage-dependent K^+ conductances with complementary functions in postsynaptic integration at a central auditory synapse. *J Neurosci* **15**, 8011–8022.

Brew HM, Hallows JL & Tempel BL (2003). Hyperexcitability and reduced low threshold potassium currents in auditory neurons of mice lacking the channel subunit Kv1.1. *J Physiol* **548**, 1–20.

Coetzee WA, Amarillo Y, Chiu J, Chow A, Lau D, Mccormack T, Moreno H, Nadal MS, Ozaita A, Pountney D, Saganich M, Vega-Saenz De Miera E & Rudy B (1999). Molecular diversity of K^+ channels. *Ann N Y Acad Sci* **868**, 233–285.

Cohen-Cory S (2002). The developing synapse: construction and modulation of synaptic structures and circuits. *Science* **298**, 770–776.

Davis GW & Bezprozvanny I (2001). Maintaining the stability of neural function: a homeostatic hypothesis. *Annu Rev Physiol* **63**, 847–869.

Desai NS, Rutherford LC & Turrigiano GG (1999). Plasticity in the intrinsic excitability of cortical pyramidal neurons. *Nat Neurosci* **2**, 515–520.

Dodson PD, Barker MC & Forsythe ID (2002). Two heteromeric Kv1 potassium channels differentially regulate action potential firing. *J Neurosci* **22**, 6953–6961.

Francis HW & Manis PB (2000). Effects of deafferentation on the electrophysiology of ventral cochlear nucleus neurons. *Hear Res* **149**, 91–105.

Friauf E & Lohmann C (1999). Development of auditory brainstem circuitry. Activity-dependent and activity-independent processes. *Cell Tissue Res* **297**, 187–195.

Keats BJ & Berlin CI (1999). Genomics and hearing impairment. *Genome Res* **9**, 7–16.

Kurima K, Peters LM, Yang Y, Riazuddin S, Ahmed ZM, Naz S, Arnaud D, Drury S, Mo J, Makishima T, Ghosh M, Menon PS, Deshmukh D, Oddoux C, Ostrer H, Khan S, Deininger PL, Hampton LL, Sullivan SL, Battey JF Jr, Keats BJ, Wilcox ER, Friedman TB & Griffith AJ (2002). Dominant and recessive deafness caused by mutations of a novel gene, TMC1, required for cochlear hair-cell function. *Nat Genet* **30**, 277–284.

Leao RN, Oleskevich S, Sun H, Bautista M, Fyffe R & Walmsley B (2004). Differences in glycinergic mIPSCs in the auditory brain stem of normal and congenitally deaf neonatal mice. *J Neurophysiol* **91**, 1006–1012.

Liu SQ & Kaczmarek LK (1998). Depolarization selectively increases the expression of the Kv3.1 potassium channel in developing inferior colliculus neurons. *J Neurosci* **18**, 8758–8769.

Mo ZL, Adamson CL & Davis RL (2002). Dendrotoxin-sensitive K^+ currents contribute to accommodation in murine spiral ganglion neurons. *J Physiol* **542**, 763–778.

Oleskevich S & Walmsley B (2002). Synaptic transmission in the auditory brainstem of normal and congenitally deaf mice. *J Physiol* **540**, 447–455.

Owen DG, Hall A, Stephens G, Stow J & Robertson B (1997). The relative potencies of dendrotoxins as blockers of the cloned voltage-gated K^+ channel, mKv1.1 (MK-1), when stably expressed in Chinese hamster ovary cells. *Br J Pharmacol* **120**, 1029–1034.

Rubel EW & Fritzsch B (2002). Auditory system development: primary auditory neurons and their targets. *Annu Rev Neurosci* **25**, 51–101.

Rudy B & Mcbain CJ (2001). Kv3 channels: voltage-gated K^+ channels designed for high-frequency repetitive firing. *Trends Neurosci* **24**, 517–526.

Schneggenburger R, Sakaba T & Neher E (2002). Vesicle pools and short-term synaptic depression: lessons from a large synapse. *Trends Neurosci* **25**, 206–212.

Shepherd RK & Hardie NA (2001). Deafness-induced changes in the auditory pathway: implications for cochlear implants. *Audiol Neurootol* **6**, 305–318.

Steel KP (1995). Inherited hearing defects in mice. *Annu Rev Genet* **29**, 675–701.

Vale C & Sanes DH (2002). The effect of bilateral deafness on excitatory and inhibitory synaptic strength in the inferior colliculus. *Eur J Neurosci* **16**, 2394–2404.

Vale C, Schoorlemmer J & Sanes DH (2003). Deafness disrupts chloride transporter function and inhibitory synaptic transmission. *J Neurosci* **23**, 7516–7524.

Van Hoesel RJ & Tyler RS (2003). Speech perception, localization, and lateralization with bilateral cochlear implants. *J Acoust Soc Am* **113**, 1617–1630.

von Hehn CA, Bhattacharjee A & Kaczmarek LK (2004). Loss of Kv3.1 tonotopicity and alterations in cAMP response element-binding protein signaling in central auditory neurons of hearing impaired mice. *J Neurosci* **24**, 1936–1940.

Wang LY, Gan L, Forsythe ID & Kaczmarek LK (1998). Contribution of the Kv3.1 potassium channel to high-frequency firing in mouse auditory neurones. *J Physiol* **509**, 183–194.

Wu SH & Kelly JB (1993). Response of neurons in the lateral superior olive and medial nucleus of the trapezoid body to repetitive stimulation: intracellular and extracellular recordings from mouse brain slice. *Hearing Res* **68**, 189–201.

Acknowledgements

We are very grateful to Dr Margaret Barnes-Davies for comments on the manuscript, and to the NHMRC of Australia for financial support.